ACADEMIC PRESS

Available online at www.sciencedirect.com

SCIENCE DIRECT®

Journal of Sound and Vibration 261 (2003) 385–402

JOURNAL OF SOUND AND VIBRATION

www.elsevier.com/locate/jsvi

Non-linear vibrations of cables considering loosening

Q. Wu, K. Takahashi*, S. Nakamura

Department of Civil Engineering, Faculty of Engineering, Nagasaki University 1-14, Bunkyo-machi, Nagasaki, Japan

Received 11 June 2001; accepted 21 May 2002

Abstract

A cable cannot resist the axial compressive force that may be induced during large amplitude vibrations. In this paper, the effect of cable loosening on non-linear vibrations of flat-sag cables is discussed by using the finite difference method that can express cable loosening. In the present method, flexural rigidity and damping of the cable are considered in the equations of motion of a cable in order to handle the numerical instability. The effect of cable loosening is evaluated explicitly in the present paper. Furthermore, non-linear vibration properties are evaluated for various parameters under periodic and step vertical loading. The effect of cable loosening on response under vertical periodic time-varying load is small and it is possible for the sag-to-span ratio to roughly equal the ratio for modal transition. The loosening under the vertical step loading in the direction opposite to the gravity appears at almost the same sag-to-span ratio.

1. Introduction

In conventional non-linear vibration analysis of cables, the equations of motion are formulated based on the assumption that the cable is a continuum resisting only axial force, and the constitutive law used is the same as truss members. In other words, cables are assumed to be able to resist both tensile and compressive axial forces [1,2]. However, the assumption cannot be applied to the case when the sum of initial and deflection-induced additional horizontal tensions becomes compressive since actual cables have no resistance against compressive force. This situation may be easily observed in non-linear vibration of cable related to strong earthquake, wind uplift, wind–rain-induced vibration [3–5], etc. Therefore, it is necessary to evaluate the effect of cable loosening in handling the non-linear vibrations of cables. An analysis considering cable loosening was carried out for stay cables in a cable stayed bridge under strong ground motion [3]. The non-linear loosening effect has also been observed in the hangers from the main cable of cable

*Corresponding author.
E-mail address: takahasi@civil.nagasaki-u.ac.jp (K. Takahashi).

0022-460X/03/$ - see front matter
PII: S0022-460X(02)01090-8

suspension bridges [6–8]. However, the mass of the cables was neglected in these analyses. Papers of research considering both loosening and mass of the cables have apparently not been published so far.

This paper attempts to examine the effect of loosening on non-linear vibrations of flat horizontal cables subjected to symmetric loading. The non-linear equations of motion of a cable formulated as a continuum are made discrete using the explicit formula of the finite difference method to solve them under the condition of the cable with no compressive resistance. A new technique adding flexural rigidity and damping is proposed to solve the divergent problem. The generation regions of compressive forces and the effect of cable loosening on the responses of cables are evaluated under vertical periodic time-varying and step loading conditions, which is a mathematical idealization for the effect of earthquake, wind uplift and wind–rain-induced vibrations.

2. Equations of motion of a cable

A horizontal cable with a uniform cross section hanging between two points as shown in Fig. 1 is analyzed. If the profile is flat, so that the sag-to-span ratio is 1:8 or less, equations of motion for non-linear vibration of a cable neglecting horizontal inertial force are obtained as follows [1]:

$$m\frac{\partial^2 w}{\partial t^2} - (H + H)\frac{\partial^2 w}{\partial x^2} + (H + \Delta H)\frac{8f}{L^2} = mg + p(x, t), \tag{1}$$

$$\Delta H = \frac{EA}{L_E}\left\{\frac{8f}{L^2}\int_0^L w\,\mathrm{d}x + \frac{1}{2}\int_0^L \left(\frac{\partial w}{\partial x}\right)^2 \mathrm{d}x\right\}, \tag{2}$$

where m is the mass per unit length, H is the initial horizontal tension induced by the dead load of the cable, ΔH is the deflection-induced additional horizontal tension, E is the Young's modulus, A is the cross-sectional area, $L_E = L\{1 + 8(f/L)^2\}$ is the length of the cable, L is the span of the cable, f is the sag of the cable, g is the gravitational acceleration, p is the vertical load intensity, w is the displacement of the cable, x is the span-wise co-ordinate of the cable and t is the time.

Although a cable is generally considered a member with no bending resistance, the effects of flexural rigidity and damping originally existing in the actual cable are considered in this paper in order to deal with cable loosening without instability in the numerical calculation. Eq. (1) is

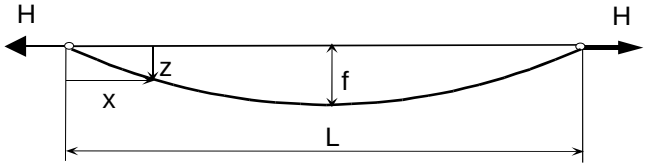

Fig. 1. Geometry of a cable.

rewritten as [9]

$$m\frac{\partial^2 w}{\partial t^2}+c\frac{\partial w}{\partial t}+EI\frac{\partial^4 w}{\partial x^4}-(H+\Delta H)\frac{\partial^2 w}{\partial x^2}+(H+\Delta H)\frac{8f}{L^2}=mg+p(x,t), \tag{3}$$

where I is the geometrical moment of inertia and c is the damping coefficient.

Making Eqs. (2) and (3) non-dimensional by the span of the cable L and the first natural circular frequency of the string ω_0, the following equations are obtained:

$$\frac{\partial^2 \bar{w}}{\partial \tau^2}+2h\omega_1\frac{\partial \bar{w}}{\partial \tau}+\frac{k^2\delta}{\pi^2}\frac{\partial^4 \bar{w}}{\partial \bar{x}^4}-\left(1+\frac{\Delta H}{H}\right)\frac{1}{\pi^2}\frac{\partial^2 \bar{w}}{\partial \bar{x}^2}+\left(1+\frac{\Delta H}{H}\right)\frac{8\gamma}{\pi^2}=\frac{8\gamma}{\pi^2}(\bar{p}(\bar{x},\tau)+1), \tag{4}$$

$$\frac{\Delta H}{H}=\frac{\lambda^2}{64}\left\{8\int_0^1\frac{1}{\gamma}\bar{w}\,\mathrm{d}\bar{x}+\frac{1}{2}\int_0^1\left(\frac{1}{\gamma}\frac{\partial \bar{w}}{\partial \bar{x}}\right)^2\mathrm{d}\bar{x}\right\}, \tag{5}$$

where $\bar{w}=w/L$ is the non-dimensional displacement in the z direction, $\bar{x}=x/L$ is the non-dimensional co-ordinate in the x direction, $\tau=\omega_0 t$ is the non-dimensional time, $\omega_0=\sqrt{H/m(\pi/L)^2}$ is the first natural circular frequency of the taut string which has no sag [1], ω_1 is the first natural circular frequency of the cable, $\bar{p}(\bar{x},\tau)=p(\bar{x},\tau)/mg$ is the non-dimensional load, h is the damping constant, $\gamma=f/L$ is the sag-to-span ratio of the cable, $k^2=EA/H$ is the ratio of the elongation stiffness to the horizontal tension of the cable (the square of the ratio of the longitudinal wave propagation velocity to the transversal wave propagation velocity), $\delta=(EI/L^2\times 1/EA)$ is the ratio of the flexural rigidity to the elongation stiffness [9] and $\lambda^2=64k^2\gamma^2/(1+8\gamma^2)$ is an Irvine parameter [1].

3. Numerical analysis method

3.1. Analysis considering loosening

Eqs. (4) and (5) are non-linear equations of motion of flat horizontal cables. Additional horizontal tensions are constant in every point of a cable, because axial inertial force of the cable is neglected based on the assumption of the flat cable. This means the total non-dimensional horizontal tension is given by $1+\Delta H/H$. In the non-linear vibration analysis for considering cable loosening, the value of total horizontal tension is made to be zero when it becomes less than zero

$$1+\frac{\Delta H}{H}=0 \quad \left(1+\frac{\Delta H}{H}<0\right). \tag{6}$$

Eq. (4) indicates that a cable without flexural rigidity and damping has no restoring force if compressive force appears in it. In this case, the vertical inertial force, the external load and the gravity are applied to the cable. In order to solve Eqs. (4) and (5) while evaluating Eq. (6), the numerical method should be used. The explicit formula of the finite difference method [10] is employed in this study. The definite integrals in Eq. (5) are calculated by Simpson's $\frac{1}{3}$ formula. The time interval for the numerical analysis should be defined to satisfy the stability condition of the scheme used.

3.2. Analysis neglecting loosening

When cable loosening is not taken into account, not only the finite difference method but also a Galerkin method can be applied to solve Eqs. (4) and (5) as described below.

The solution of Eq. (4) is assumed as follows:

$$\bar{w}(\bar{x},\tau)=\sum_{i=1}^{\infty}T_i(\tau)W_i(\bar{x}), \tag{7}$$

where $T_i(\tau)$ is the unknown time function and $W_i(\bar{x})$ is the co-ordinate function.

In this paper, the natural modes of linear vibrations of the cable without the flexural rigidity are used as the co-ordinate functions [1]. Only the symmetric modes that produce additional horizontal tension are considered in the present analysis. The co-ordinate function in this case is given as

$$W_i(\bar{x})=1-\tan\frac{\bar{\omega}_i\pi}{2}\sin\bar{\omega}_i\pi\bar{x}-\cos\bar{\omega}_i\pi\bar{x}, \tag{8}$$

where $\bar{\omega}_i=\omega_i/\omega_0$ is the ith non-dimensional natural circular frequency and obtained by the following equation:

$$\tan\frac{\bar{\omega}_i\pi}{2}=\frac{\bar{\omega}_i\pi}{2}-\frac{4}{\lambda^2}\left(\frac{\bar{\omega}_i\pi}{2}\right)^3. \tag{9}$$

Substituting Eq. (7) into Eqs. (4) and (5) and employing a Galerkin method, the non-linear ordinary differential equations with respect to the time function $T_m(\tau)$ are obtained as follows:

$$M_m\ddot{T}_m(\tau)+2h\omega_1M_m\dot{T}_m(\tau)+\frac{k^2\delta}{\pi^2}\sum_{i=1}^{\infty}A_m^iT_i(\tau)-\left(1+\frac{\Delta H}{H}\right)\frac{1}{\pi^2}\sum_{i=1}^{\infty}B_m^iT_i(\tau)$$
$$+\left(1+\frac{\Delta H}{H}\right)\frac{8\gamma}{\pi^2}K_m-\frac{8\gamma}{\pi^2}K_m\{\bar{p}(\bar{x},\tau)+1\}=0, \tag{10}$$

$$\frac{\Delta H}{H}=\frac{\lambda^2}{64}\left\{\frac{8}{\gamma}\sum_{i=1}^{\infty}K_iT_i(\tau)-\frac{1}{2\gamma^2}\sum_{i=1}^{\infty}\sum_{j=1}^{\infty}B_j^iT_i(\tau)T_j(\tau)\right\}, \tag{11}$$

where $M_m=\int_0^1W_m^2(\bar{x})\,\mathrm{d}\bar{x}$, $A_m^i=\int_0^1(\mathrm{d}^4W_i(\bar{x})/\mathrm{d}\bar{x}^4)W_m(\bar{x})\,\mathrm{d}\bar{x}$, $B_m^i=\int_0^1(\mathrm{d}^2W_i(\bar{x})/\mathrm{d}\bar{x}^2)W_m(\bar{x})\,\mathrm{d}\bar{x}$ and $K_m=\int_0^1W_m(\bar{x})\,\mathrm{d}\bar{x}$ are the constants dependent on the modal shapes of the linear problem by a Galerkin method.

4. Analytical condition

The loads used in this paper are uniformly distributed periodic time-varying and uniformly distributed step vertical loads.

Periodic time-varying vertical load is expressed in the form of following equation:

$$\bar{p}(\bar{x},\tau)=p_0\sin\{(\Omega/\omega_1)\tau\}, \tag{12}$$

where Ω is the circular frequency of the load and its value is set to be the same as the first symmetrical circular frequency of the linear cable. The load intensity p_0 is non-dimensionalized by the cable weight per unit length. The initial displacement and velocity of the cable are made to be zero. The number of divisions of a cable is 100, that is, $\Delta\bar{x} = 0.01$. In order to satisfy the stability condition, the time interval must be less than 2.5×10^{-5} and 1.0×10^{-5} is used here.

5. Responses under periodic time-varying vertical loading

5.1. Accuracy of the finite difference method

In order to examine the accuracy of the finite difference method, an eigenvalue analysis is done by the finite difference method, in which flexural rigidity and damping are neglected (the ratio of flexural rigidity to the elongation stiffness $\delta = 0$, the damping constant $h = 0$), and the results are compared with the symmetric eigenvalues obtained by Irvine's equation (Eq. (9)). The relationship between non-dimensional symmetric natural frequencies and parameter λ^2 is shown in Fig. 2. The antisymmetric eigenvalues which are the same as those of the strings are also shown in Fig. 2. The results obtained by the finite difference method overlap with those by Irvine's equation. These two solutions give the same results.

For the case in which the compressive forces do not appear, the time histories obtained by the finite difference method and a Galerkin method (10 modes approximation) are shown in Figs. 3(a)–(c). Figs. 3(a) and (b) are time histories of the displacement at the center point and the total horizontal tension ($\delta = 0$ and $h = 0$), respectively. The two time histories overlap each other and coincide very well in both displacement and tension. The modal shapes are kept smooth and the same in compression and tension sides as shown in Fig. 3(c). Therefore, it is possible to use the finite difference method to evaluate the response characteristics of the cable without cable loosening even if flexural rigidity and damping are not considered.

Fig. 4 shows the responses with compressive force in the cable. The calculation results by the finite difference method and the Galerkin method are illustrated in the figure. Time histories

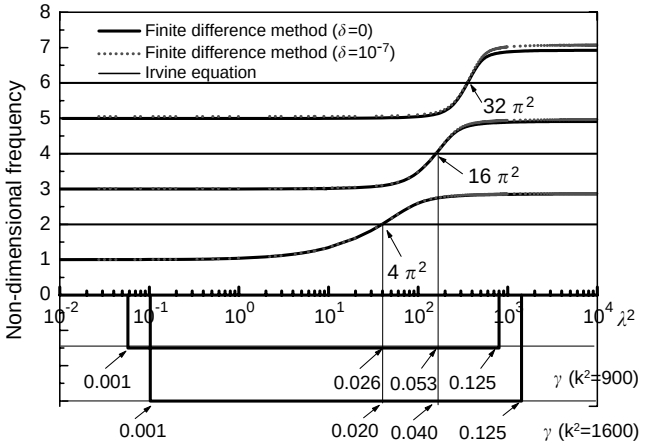

Fig. 2. Natural frequencies of a cable.

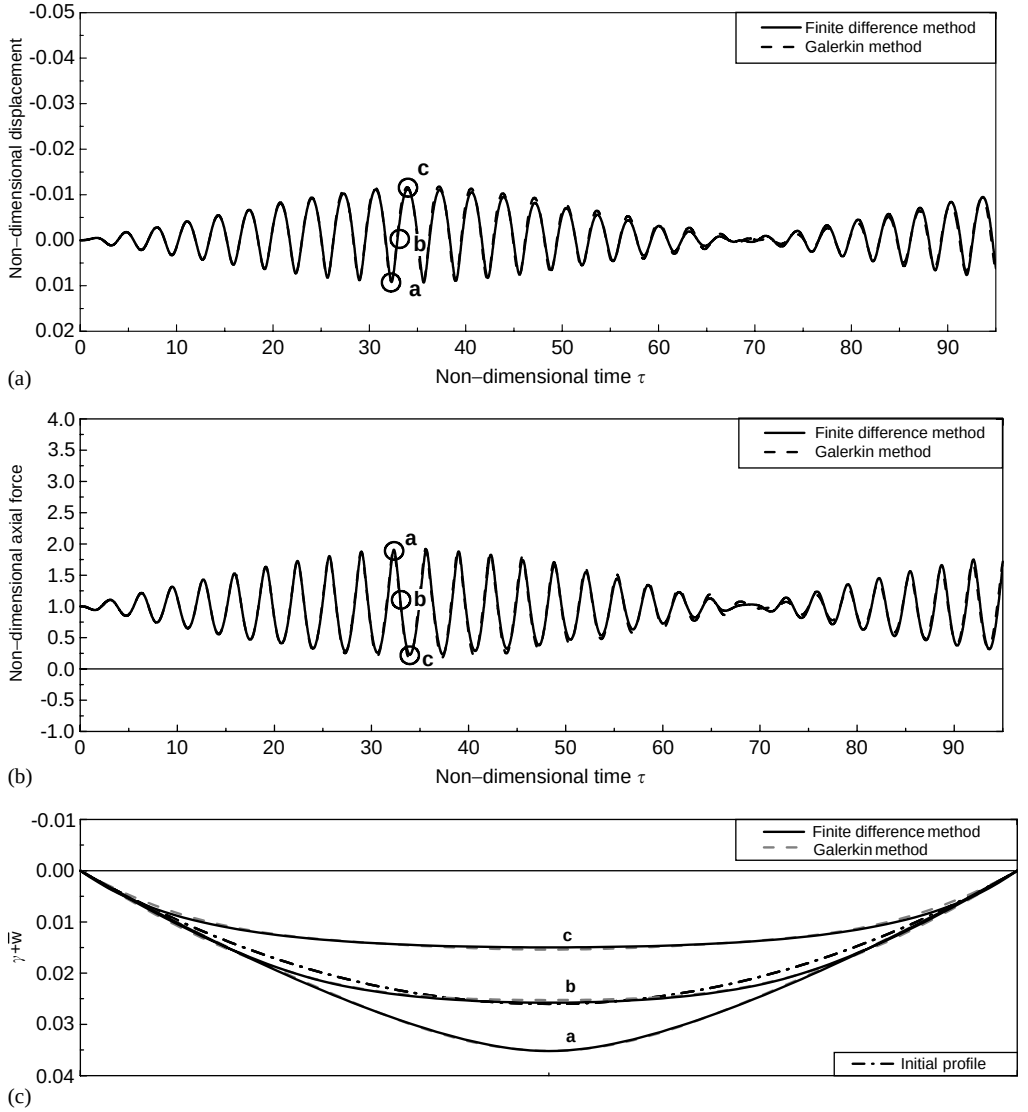

Fig. 3. Time histories of: (a) displacement $\bar{w}$ at center point, (b) horizontal axial force $1+\Delta H/H$, and (c) space shapes of a cable for $\gamma=0.026$, $k^2=900$, $p_0=0.05$, $\delta=0$ and $h=0$. Notations a, b and c correspond to the maximum, zero and minimum displacements at the center of the cable.

obtained by the finite difference method with and without consideration of cable loosening are compared in Figs. 5(a) and (b). The corresponding space shapes of the cable are shown in Fig. 5(c). Notations a, b and c correspond to the maximum, zero and minimum displacements at the center of the cable.

The compressive force appears at about the non-dimensional time $\tau=8$ first, as shown in Fig. 4(b). The difference between the finite difference method and a Galerkin method can be seen

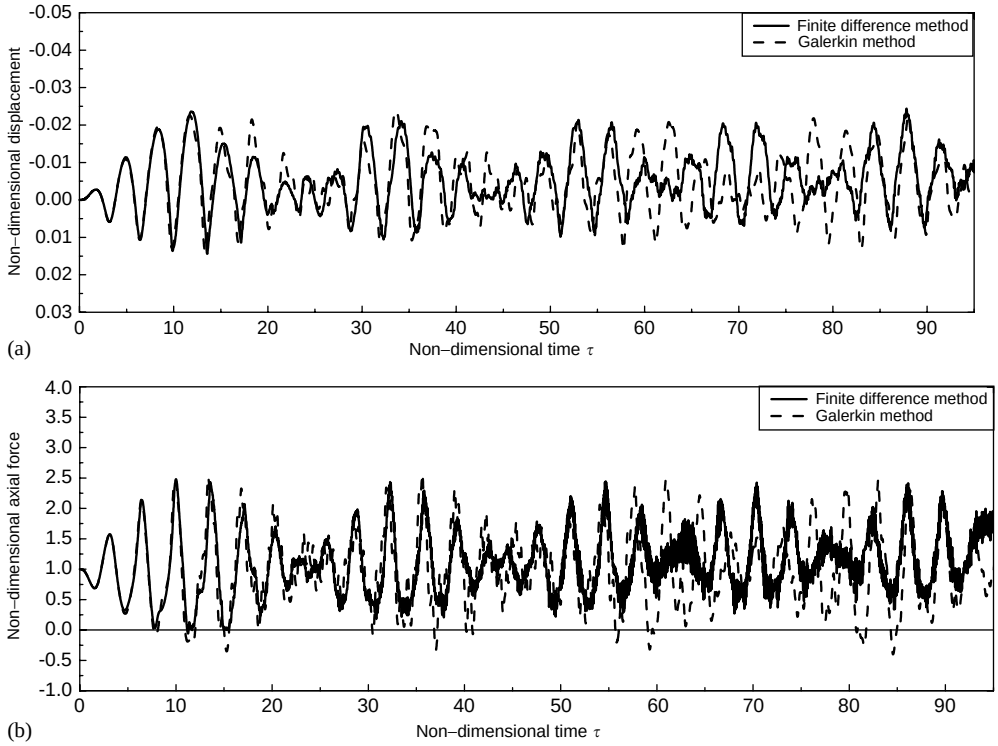

Fig. 4. Time histories of a cable for $\gamma = 0.026$, $k^2 = 900$, $p_0 = 0.27$, $\delta = 0$ and $h = 0$: (a) displacement $\bar{w}$ at center point and (b) horizontal axial force $1 + \Delta H/H$.

after this time. A higher mode shape with discontinuity of the angle is observed in the space shape of the cable at point c in Figs. 5(a) and (b) as shown in Fig. 5(c). This can be the cause of the difference. Space shapes obtained by the finite difference method have such higher mode with angular discontinuities when the total horizontal tension is close to zero. Their positions change with the number of divisions of the cable in the analysis. The space shapes seem to become discontinuous in the cable relaxations since the solution of Eq. (1) by the finite difference method does not need to satisfy the continuity of the deflection angle of the cable.

In addition, the responses of the cable diverge like Figs. 5(a) and (b) if cable loosening is considered. It may be caused by the occurrence of larger discontinuous deflection angles in the space shapes of the cable. These discontinuous deflection angles bring out the additional horizontal tension and diverge the response. Therefore, it is impossible to use the finite difference method to calculate the responses of cables with loosening.

5.2. *Analysis considering flexural rigidity and damping*

In order to prevent the cable from undergoing the vibration components of higher modes with discontinuous angles described in the above section, the ratio of flexural rigidity to elongation stiffness δ and damping constant h, which cables originally have, are considered in the analysis by

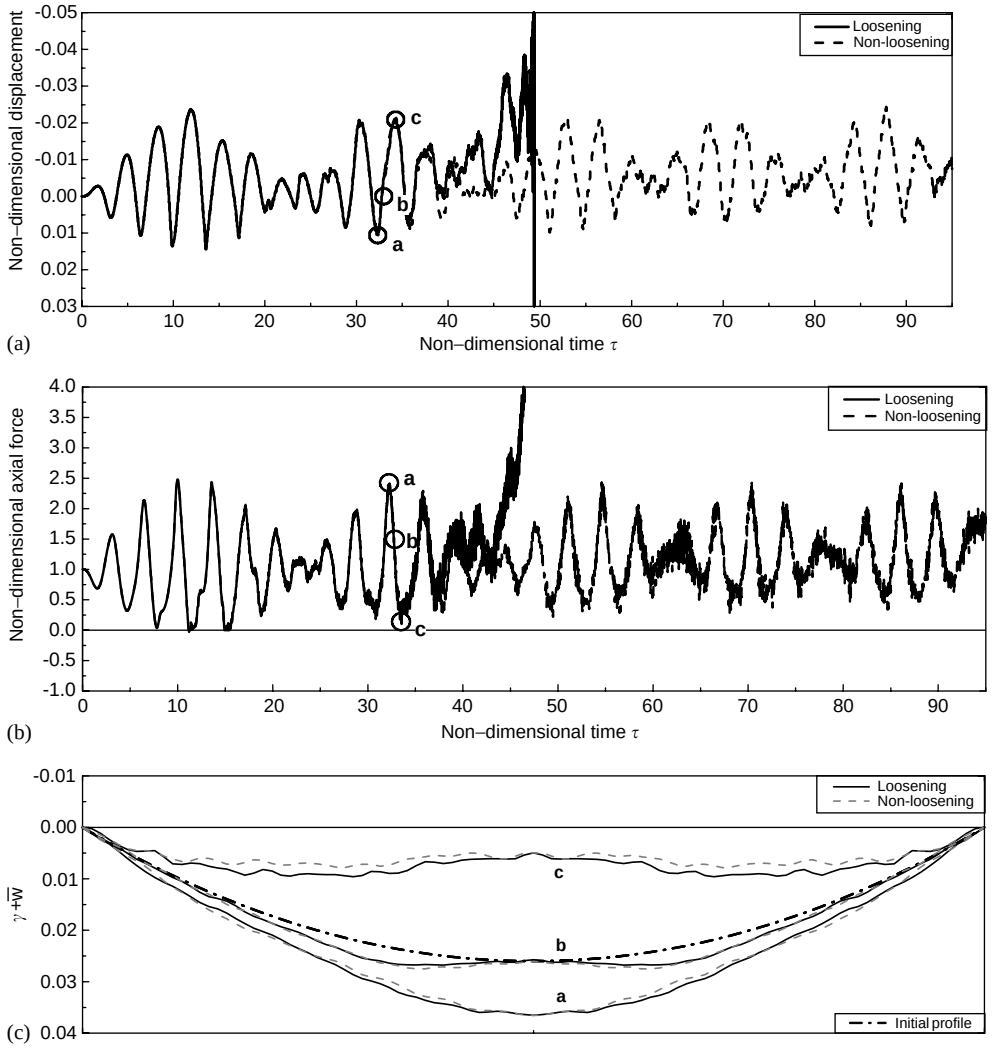

Fig. 5. Time histories of: (a) displacement $\bar{w}$ at center point, (b) horizontal axial force $1+\Delta H/H$, and (c) space shapes of a cable for $\gamma = 0.026$, $k^2 = 900$, $p_0 = 0.27$, $\delta = 0$ and $h = 0$.

the finite difference method. The effect of flexural rigidity δ on the vibration of the cable becomes large in the case of the higher mode with change of the curvature of the cable [9]. From this fact, the rigidity δ is taken into consideration in the present analysis. The direct time integration α-method presented by Hilber et al.[11] improves numerical stability by algorithm damping higher modes, while the flexural rigidity and damping, which cables possess as physical properties influencing on higher modes, are taken into consideration in the present paper as shown in Eq. (3).

The natural frequencies of cables in the case of $\delta = 10^{-7}$ are also plotted in Fig. 2. Results in the case of chosen value $\delta = 10^{-7}$ overlap with those in the case of $\delta = 0$ except the third symmetric mode where $\lambda^2 > 4 \times 10^2$. The effect of the flexural rigidity on the lower frequencies is very small in

the case of $\delta = 10^{-7}$. For the same case, the responses obtained by both the finite difference method neglecting cable loosening and the Galerkin method are shown in Fig. 6. It can be seen that the two responses show good agreement.

The responses ($\delta = 10^{-7}$ and $h = 0.001$, the other parameters are the same as Fig. 5) are shown in Figs. 7(a)–(c). The vibration components of higher modes with discontinuous angles are excluded and the space shapes become smooth, as shown in Fig. 7(c). When these two parameters are considered, the responses using the finite difference method become difficult to diverge and it is possible to calculate them even if the compressive forces appear in the cable. So, the response characteristics of cables with possible loosening can be clarified by considering the flexural rigidity and damping of the cables in the analysis by the finite difference method. It is numerically confirmed that the current technique of adding flexural rigidity and damping solves the divergent problem.

The higher mode vibration without discontinuity becomes more predominant than Fig. 5(c) in the space shapes of the cable in the compression side. These space shapes make it difficult to generate the compressive force in the cable.

It can also be confirmed that space shapes change with the amplitudes of cables. Figs. 8–10 show the time histories when the load intensities are 1.5, 2.0 and 3.0 times of Fig. 7, respectively.

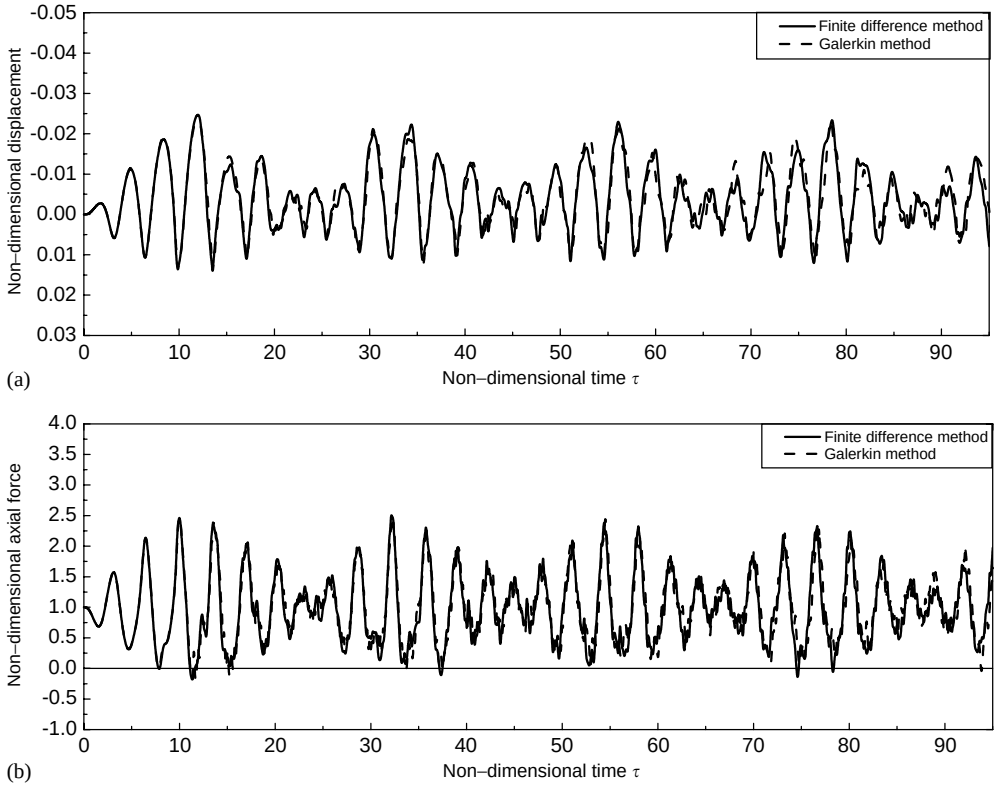

Fig. 6. Time histories of a cable for $\gamma = 0.026$, $k^2 = 900$, $p_0 = 0.27$, $\delta = 10^{-7}$ and $h = 0.001$: (a) displacement $\bar{w}$ at center point and (b) horizontal axial force $1 + \Delta H/H$.

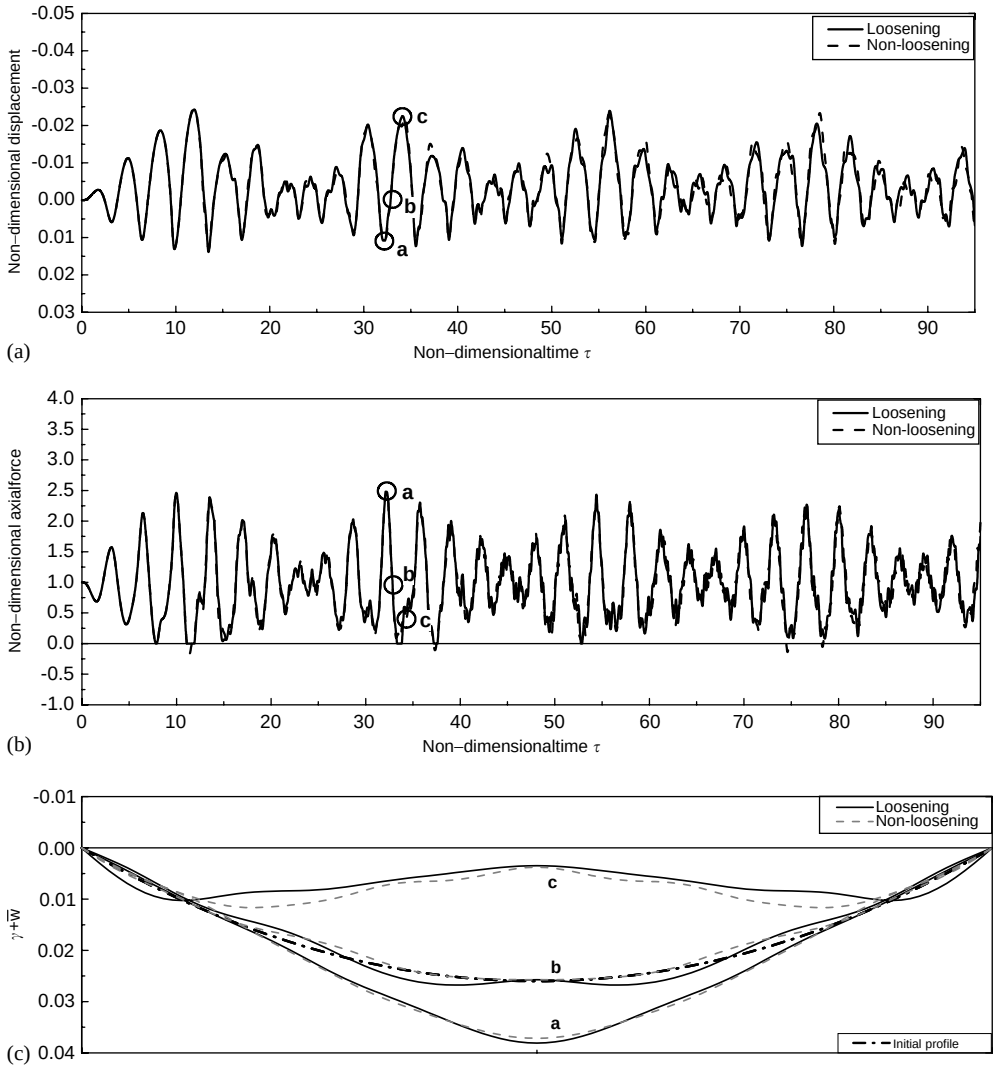

Fig. 7. Time histories of: (a) displacement $\bar{w}$ at center point, (b) horizontal axial force $1 + \Delta H/H$, and (c) space shapes of a cable for $\gamma = 0.026$, $k^2 = 900$, $p_0 = 0.27$, $\delta = 10^{-7}$ and $h = 0.001$.

The negative displacements, the compressive forces and the compression generated regions do not increase very much from the values shown in Fig. 7 although those in the tensile region do obviously. The reason for this can be advanced that cables keep the space shapes which are difficult to generate the compressive forces as shown in Figs. 7(c), 8(c), 9(c) and 10(c).

The effect of loosening on the responses of cables under the periodic vertical loadings is small for the numerical example in this study because the compression generated regions are narrow.

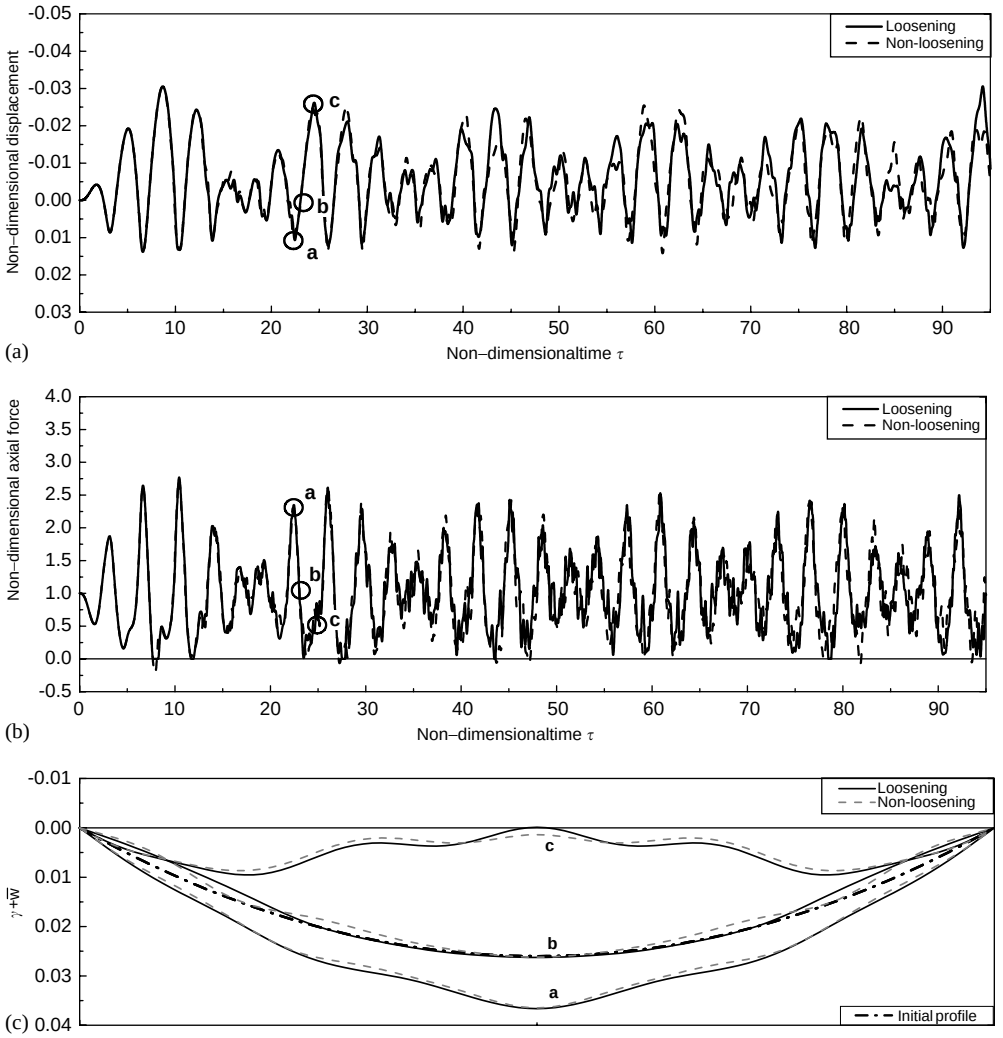

Fig. 8. Time histories of: (a) displacement $\bar{w}$ at center point, (b) horizontal axial force $1+\Delta H/H$, and (c) space shapes of a cable for $\gamma = 0.026$, $k^2 = 900$, $p_0 = 0.27 \times 1.5$, $\delta = 10^{-7}$ and $h = 0.001$.

5.3. *Minimal loads and amplitudes to generate compressive forces in the cable*

The relationship between minimal load intensity p_0 to generate compressive forces in the cable and parameter λ^2 is shown in Fig. 11. For reference, the sag-to-span ratio γ is shown in the cases of $k^2 = 900$ and 1600.

The compressive force begins to appear from near $\lambda^2 = 2.47\pi^2$ and p_0 has the local minimum near $\lambda^2 = 4\pi^2$ which corresponds to the mode transition region from the first to the second symmetrical vibration (see Fig. 2). Next, it has the minimum near $\lambda^2 = 16\pi^2$. This sag-to-span ratio γ is also correspondent with the mode transition region from the second to the third

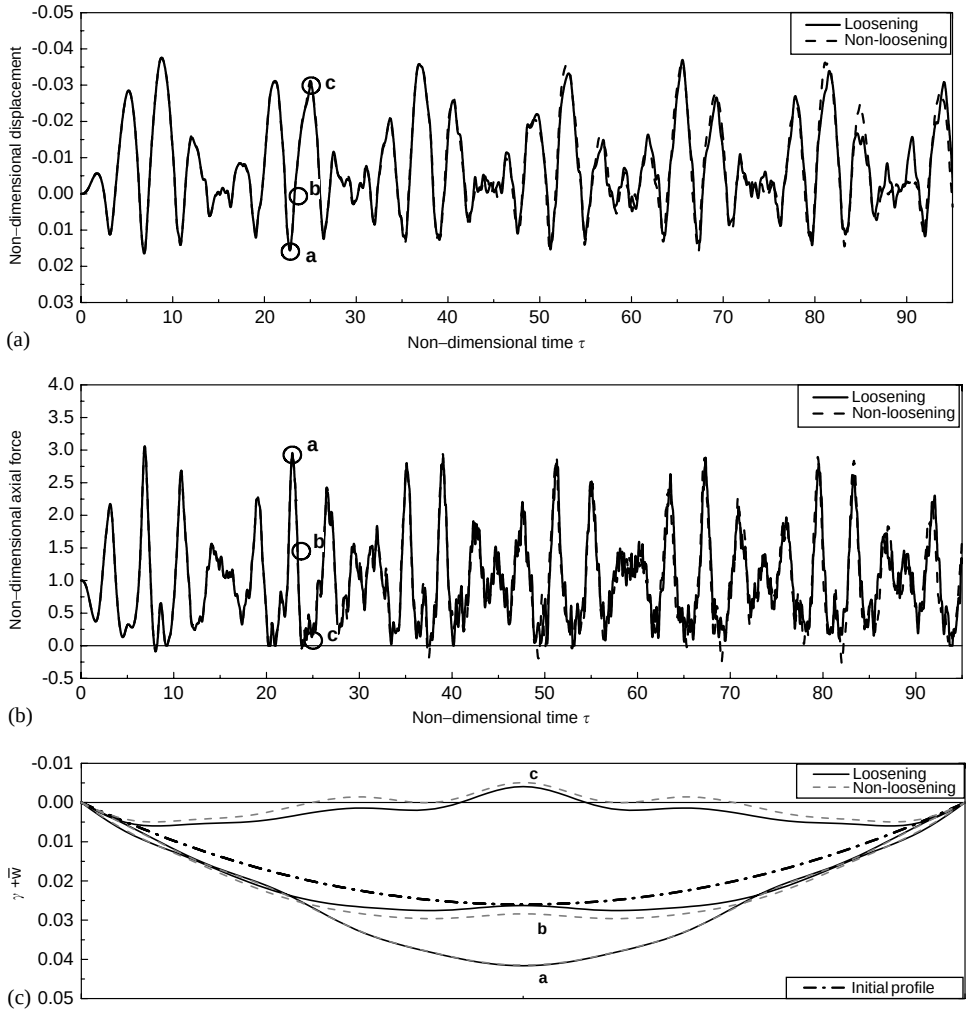

Fig. 9. Time histories of: (a) displacement $\bar{w}$ at center point, (b) horizontal axial force $1+\Delta H/H$, and (c) space shapes of a cable for $\gamma = 0.026$, $k^2 = 900$, $p_0 = 0.27 \times 2.0$, $\delta = 10^{-7}$ and $h = 0.001$.

symmetrical vibration in Fig. 2. Like this, the cables with the sag-to-span ratio γ corresponding to the natural mode transition region can be easily compressive.

Fig. 12 represents the non-dimensional compression causing displacement and the sag-to-span ratio γ relationship. When the non-dimensional displacement of cables is about 70% of the sag-to-span ratio γ, the compressive force begins to appear. Although the displacement fluctuates as the sag-to-span ratio γ increases, the general tendency of decrease in the displacement with increase of sag-to-span ratio γ can be seen.

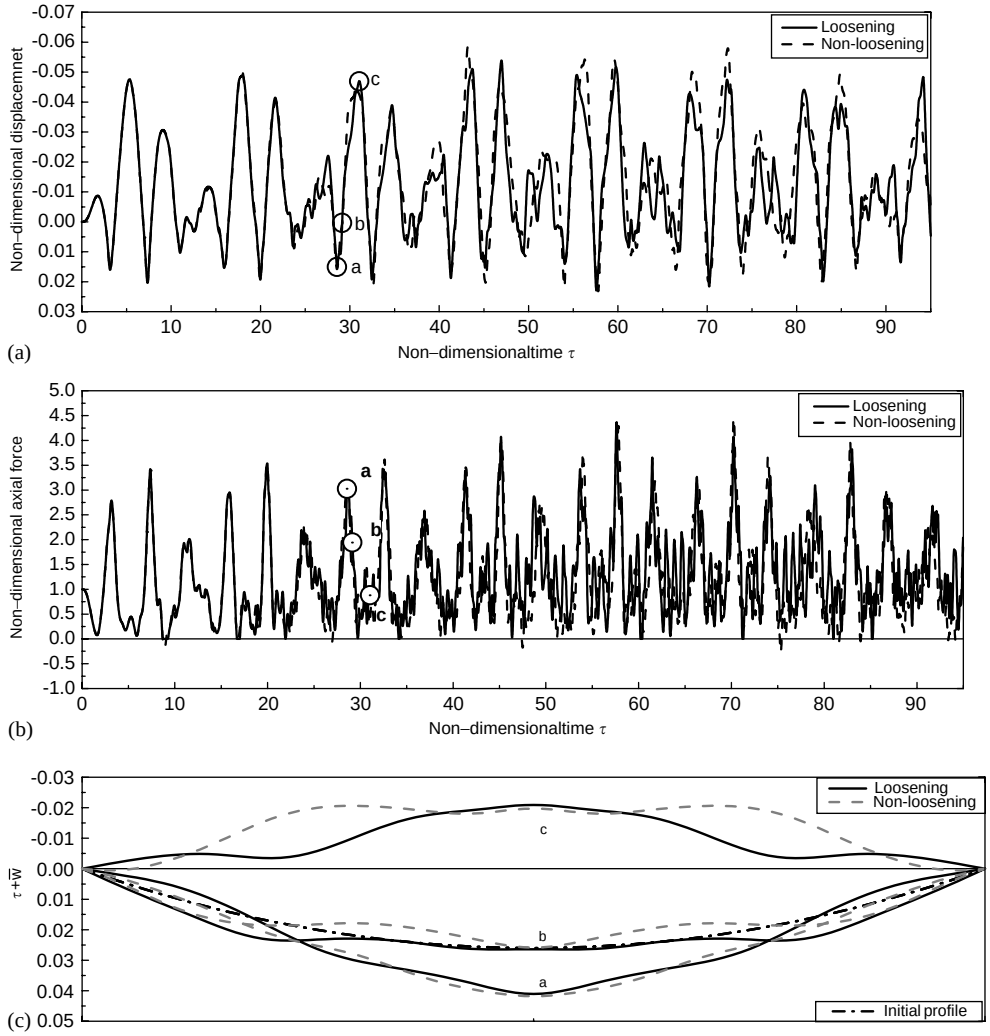

Fig. 10. Time histories of: (a) displacement $\bar{w}$ at center point, (b) horizontal axial force $1 + \Delta H/H$, and (c) space shapes of a cable for $\gamma = 0.026$, $k^2 = 900$, $p_0 = 0.27 \times 3.0$, $\delta = 10^{-7}$ and $h = 0.001$.

The minimal sag-to-span ratio which can generate the compressive force and the compression causing displacement decreases with the increase of the ratio of elongation stiffness to horizontal tension k^2.

6. Responses under step vertical loading

The response characteristics of the cable under the step vertical loading $\bar{p}(\bar{x}, \tau) = p_0$ in the direction opposite to the gravity are clarified in this section. This may be the easiest way to generate the compressive forces in the cable.

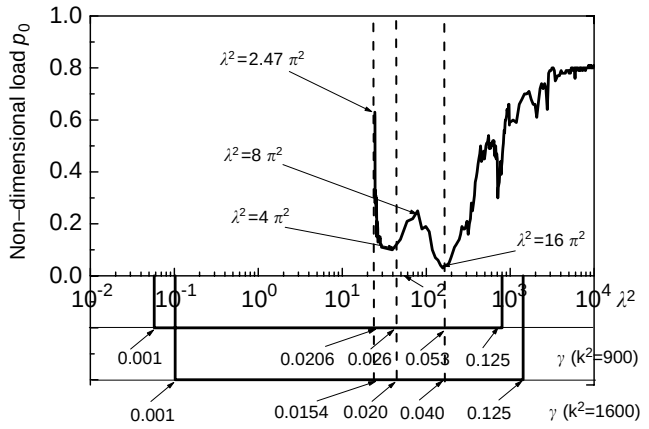

Fig. 11. Relationship between loads p_0 in which the compressive force appears and Irvine parameter λ^2 for $\delta = 10^{-7}$ and $h = 0.001$.

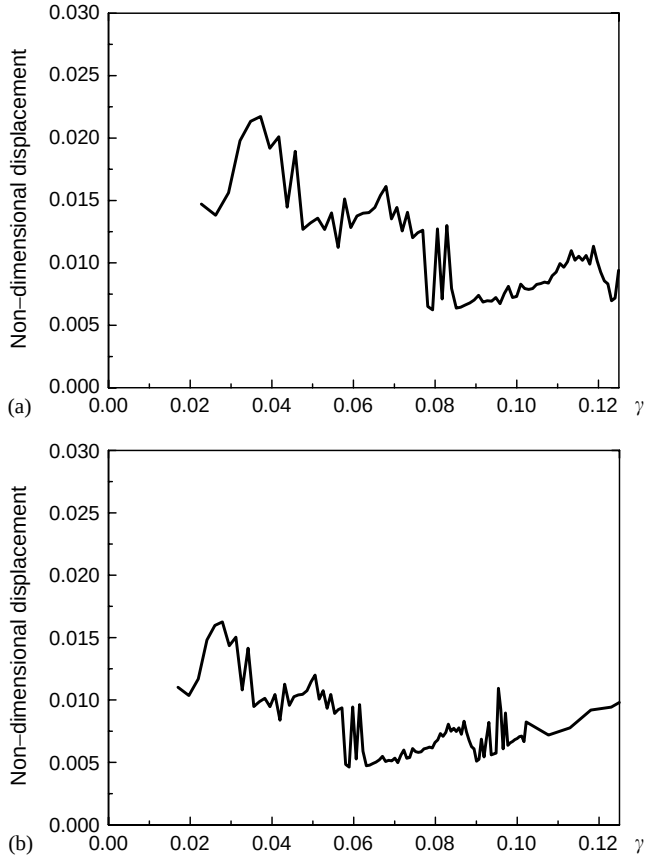

Fig. 12. Relationship between displacement $\bar{w}$ in which the compressive force appears and sag-to-span ratio γ for $\delta = 10^{-7}$ and $h = 0.001$: (a) $k^2 = 900$ and (b) $k^2 = 1600$.

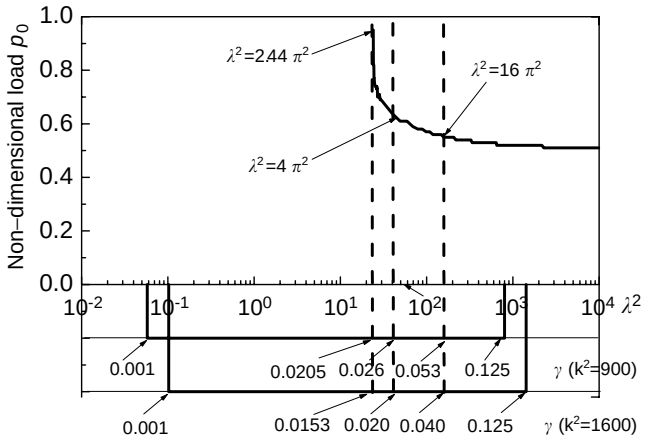

Fig. 13. Relationship between step loads p_0 in which the compressive force appears and Irvine parameter λ^2 for $\delta = 10^{-7}$ and $h = 0.001$.

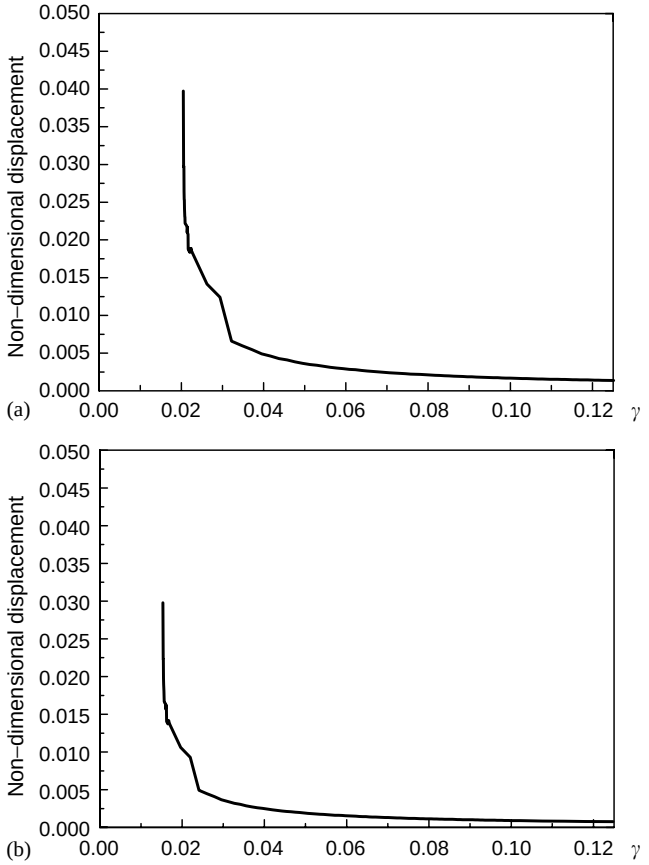

Fig. 14. Relationship between displacement $\bar{w}$ in which the compressive force appears and sag-to-span ratio γ for $\delta = 10^{-7}$, $h = 0.001$ and step load: (a) $k^2 = 900$ and (b) $k^2 = 1600$.

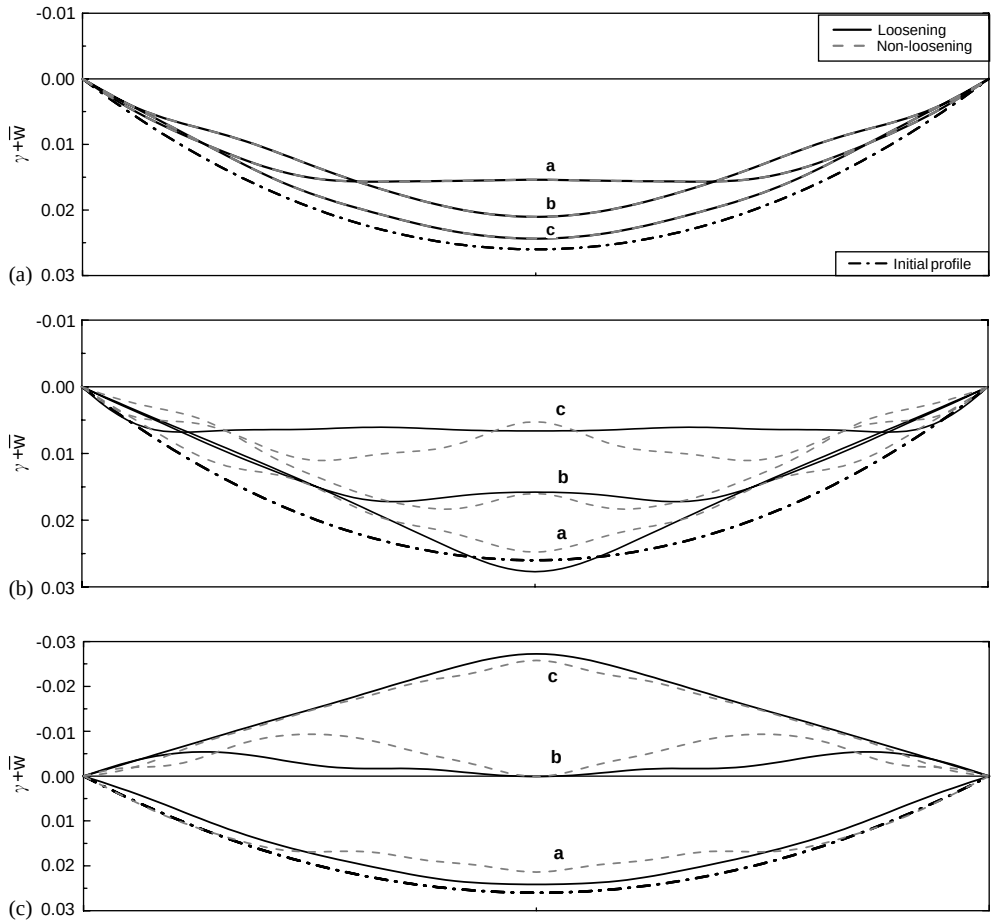

Fig. 15. Space shapes of a cable under step loads for $\gamma = 0.026$, $k^2 = 900$, $\delta = 10^{-7}$ and $h = 0.001$: (a) $p_0 = 0.6$, (b) $p_0 = 0.8$, and (c) $p_0 = 1.0$.

Fig. 13 shows the relationship between the compression producing step load intensity p_0 and parameter λ^2. The compressive force begins to appear near $\lambda^2 = 2.44\pi^2$, which is almost the same value under periodic vertical loading. The load intensity gradually decreases with increase of λ^2. The non-dimensional compression producing displacement monotonically decreases with the increase of sag-to-span ratio γ as shown in Fig. 14. Space shapes in the cases of $p_0 = 0.6$, 0.8 and 1.0 are shown in Figs. 15(a)–(c), respectively. The response of displacement at the center point, the horizontal axial force and the power spectral density for $p_0 = 0.8$ are shown in Figs. 16(a)–(c). The effect of cable loosening lengthens the period of the cable as shown in Fig. 16(c).

7. Concluding remarks

In this paper, numerical analysis using the finite difference method was carried out in order to discuss the effect of cable loosening on dynamic behaviors of horizontal flat cables. An analysis

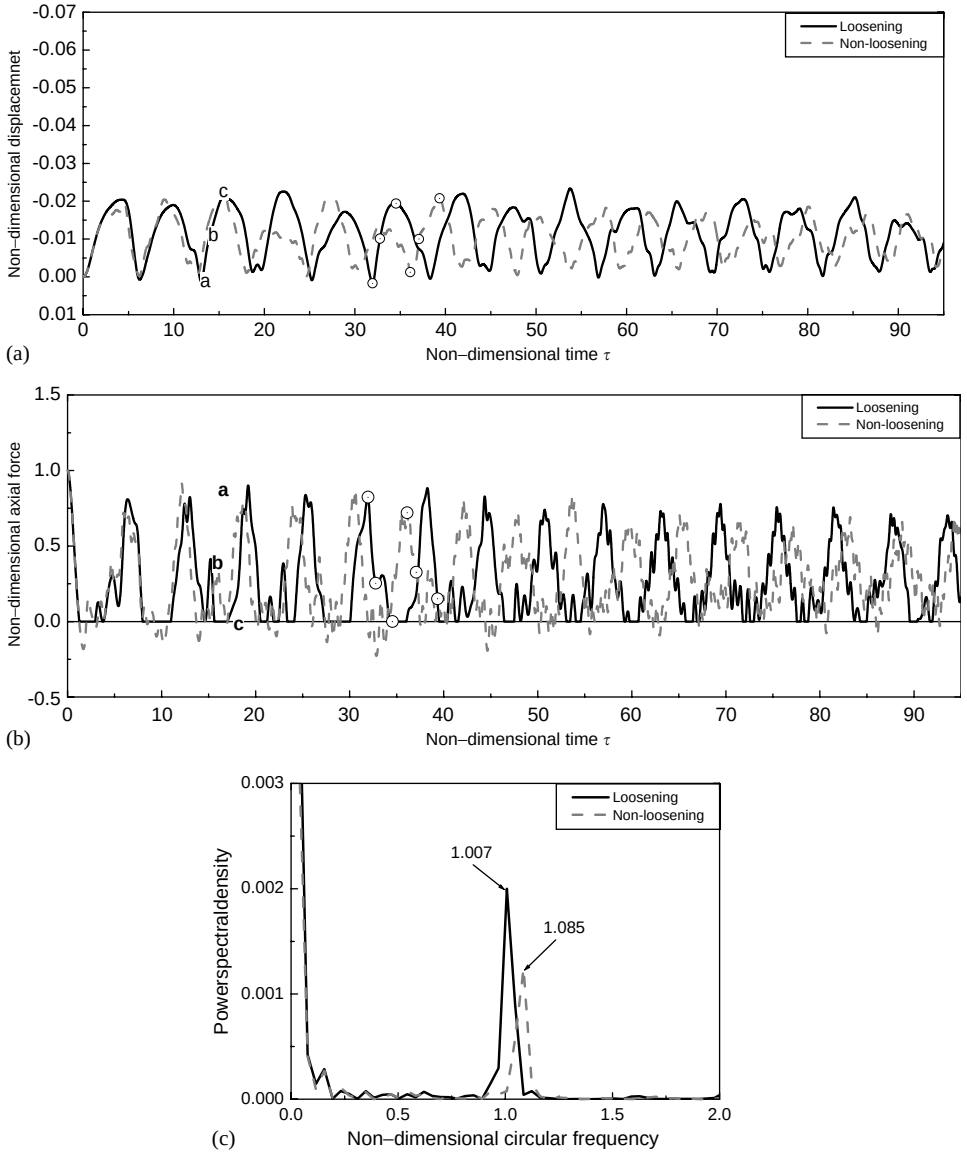

Fig. 16. Time histories under step loads of: (a) displacement $\bar{w}$ at center point, (b) horizontal axial force $1 + \Delta H/H$, and (c) power spectral density of a cable for $\gamma = 0.026$, $k^2 = 900$, $p_0 = 0.80$, $\delta = 10^{-7}$ and $h = 0.001$.

method of non-linear vibration of cables considering flexural rigidity and damping is proposed in order to handle possible loosening. By this method, the dynamic characteristics of cables with possible loosening are spelled out explicitly and clarified. Main findings of this study can be summarized as follows:

(1) The loosening is easy to appear in the cables with the sag-to-span ratio corresponding to the mode transition region from the lower mode to the higher mode under periodic vertical

loading. The non-dimensional compression producing displacement depends on the sag-to-span ratio and the ratio of the elongation stiffness to the horizontal tension. The compressive force appearing region in the time history of the cable response is narrow since the higher modes become predominant in the space shapes of the cable in the compression to reduce the compressive force. Therefore, the effect of loosening on the response amplitudes and frequencies of cables is not predominant.

(2) The loosening of the cable under the vertical step loading in the direction opposite to the gravity appears at the almost same sag-to-span ratio under periodic vertical loading. The non-dimensional compression producing displacement decreases with the increase of the sag-to-span ratio.

References

[1] H.M. Irvine, Cable Structures, The Massachusetts Institute of Technology Press, Cambridge, MA, 1981.
[2] H. Yamaguchi, M. Ito, Linear theory of free vibrations of an inclined cable in three dimensions, Proceedings of the Japan Society of Civil Engineers 286 (1979) 29–38 (in Japanese).
[3] Q. Wu, K. Takahashi, S. Nakamura, The effect of loosening of cables on seismic response of the cable-stayed bridge, 50th National Congress Theoretical and Applied Mechanics, 2001, pp. 229–230 (in Japanese).
[4] M. Matsumoto, H. Ishizaki, M. Kitazawa, J. Aoki, D. Fujii, Cable aerodynamics and its stabilization, Proceedings of the International Symposium on Cable Dynamics, 1995, pp. 289–296
[5] A. Honda, Y. Yamanaka,T. Fujiwara, Wind tunnel test on rain-induced vibration of the stay-cable, Proceedings of the International Symposium on Cable Dynamics, 1995, pp. 255–262.
[6] A.C. Lazer, P.J. Mckenna, Large-amplitude periodic oscillations in suspension bridges: some new connections with non-linear analysis, SIAM Review 32 (1990) 537–578.
[7] I. Peterson, Rock and roll bridge: a new analysis challenges the common explanation of a famous collapse, Science News 137 (1990) 344–346.
[8] V. Sepe, G. Augusti, A deformable section model for the dynamics of suspension bridges, Part I: model and linear response, Wind and Structures 4 (2001) 1–18.
[9] H. Yamaguchi, T. Miyata, M. Ito, Free in-plane vibration of a cable with bending rigidity, Proceedings of the Japan Society of Civil Engineers 319 (1982) 13–19 (in Japanese).
[10] W.F. Ames, Numerical Methods for Partial Differential Equations, 2nd Edition, Academic Press, New York, 1977.
[11] H.M. Hilber, T.J.R. Hughes, R.L. Taylar, Improved numerical dissipation for time integration algorithms in structural dynamics, Earthquake Engineering and Structural Dynamics 5 (1977) 283–292.